Stopping of Protons - Improved Accuracy of the UCA Model

G. Schiwietz[*,1] and P.L. Grande[2]

[1] Helmholtz-Zentrum Berlin f. Materialien u. Energie, Hahn-Meitner-Platz 1, 14109 Berlin, Germany

[2] Uni. Federal do Rio Grande do Sul, Av. Bento Gonçalves 9500, 91501-970 Porto Alegre, RS, Brazil

Abstract

Recent theoretical developments in the **u**nitary **c**onvolution **a**pproximation (UCA) for electronic energy losses of bare and screened ions are presented. Examples are given for proton beams and rare-gas targets. For gas targets there exists a sufficient amount of experimental data on charge exchange, for pinpointing the largely unknown stopping-power contribution of electron-capture processes at low and intermediate energies.

PACS numbers: *34.50.Bw , 34.50. Fa,34.10.+x, 61.85.+p*

Keywords: *ion energy loss, gas target, non-perturbative effects, cross sections, energy transfer, stopping power, low energies*

[*] corresponding author, email: schiwietz(at)helmholtz-berlin.de

I. Introduction

Theoretical investigations of the energy losses of charged particles started with relatively simple classical[1, 2] models and later quantum mechanical[3, 4] theories. These early attempts were concentrating on ionization processes. In this work, we try to consider most important *electronic energy-loss* processes.[5] We will use the term "fast projectiles" to indicate speeds beyond the orbital velocities of most of the weakly bound electrons (say $E_p/M_p >> 500$ *keV/u*), where many electron shells contribute to the ion energy-loss. With "slow projectiles" we mean that the projectile interacts mainly with the valence-band, corresponding to $E_p/M_p << 20$ *keV/u*.

The transfer of target electrons to bound projectile state (electron capture) triggers so-called *capture-and-loss cycles*, where the captured electron is lost by the projectile in subsequent collisions, involving a projectile energy-loss as well. The influence of electron capture depends strongly on the projectile charge state and, specifically at low velocities, on matching conditions for the electronic energy levels of target and projectile (resonant or non-resonant electron capture).[6] Uncertainties of the (extended) Firsov model might be one of the reasons why some models suggest that the influence of electron capture at low velocities is enormous[7], while other authors[8] assume that the neglect of charge exchange may not be a serious omission.

This paper is focused on developments of the **U**nitary **C**onvolution **A**pproximation (***UCA***) and on partial ion energy-loss cross sections for specific projectile charge-states and energy-transfer processes, extending the range of validity to projectile energies far below 100 keV/u. Further, we present theoretical CasP energy-loss results in comparison to other theoretical results and experimental data. We will show that electron-capture processes may not be neglected for gas targets, not even for asymmetrical collision systems. If not indicated otherwise, atomic units ($e=m_e=\hbar=1$ a.u.) are used throughout the paper.

II. New Developments of the UCA Model

The **CasP** computer code (**C**onvolution **a**pproximation for **s**wift **P**rojectiles) includes many different modes of operation.[9] The program makes use of the convolution approximation (either the **perturbative convolution approximation *PCA***[10, 11] or the more advanced ***UCA***[12, 13]). The physical inputs of the program[9] are the projectile velocity, the projectile-screening potential, the target-electron density distribution (tabulated using our Hartree-Fock-Slater code[14, 15]) and the target oscillator-strengths. The code is based on an exact matching of the quantum mechanical mean electronic energy transfers for the asymptotic regions of small and large impact parameters. The code is not restricted to Coulombic point charges as screening of the projectile charge is fully included.[16] This means that we use the so-called charge-state approach[17, 18] and average all energy losses over the projectile charge-state fraction (including electron-loss processes).

Although there is some knowledge on the charge-state evolution[19], even the most advanced current theoretical charge-state treatments involve a somewhat limited accuracy and limited parameter ranges.[20] Accurate charge-state fits for ions in solids and gases[21] are still a necessary ingredient for accurate stopping-power calculations. For H+He and H+Ne we incorporate now directly the experimental charge-state fractions (not the fit formula[21] as used for all other systems), since both targets involve the most strongly bound valence electrons and deviate (for protons) in their charge-state evolution from other systems.

A model with very general applicability is the UCA as developed by the present authors.[10, 12] It has undergone many test phases and has been continuously improved over the years. At high ion velocities, *1st order perturbation* theory for excitation and ionization, also named *1st-order semi-classical approximation*[4, 22, 23] or equivalently *plane-wave Born approximation*[24] *(PWBA)* or *Bethe theory* (don't mix up with the simplified Bethe formula) [3, 17, 25] is often used. The UCA model approaches the PWBA at high speeds and includes a simple relativistic correction[26], extending its range-of-validity up to several 100 MeV/u. Similar to most models

for transitions from localized electronic states, CasP is based on the impact-parameter method[22] and on the independent-electron picture. The only current energy-loss theory that involves no further approximations, is the *atomic-orbital coupled-channel* (*AO-CC*) theory[27, 28, 29] and may thus even be applied to slow ions. Further corrections and ingredients extend also the UCA's range-of-validity towards lower energies as will be discussed in the following sections.

II.1 Barkas Correction

At intermediate energies, the *Barkas (polarization-) effect*[30, 31] (dominated by $Z_p^{\,n}$ contributions with $n=3$) is important for an accurate stopping-power prediction. At large impact parameters, it is related to an energy-loss enhancement due to an attraction of target electrons by a positive projectile-ion charge. Similar to the projectile induced binding effect at close collisions (described e.g. in the perturbed-stationary-state theory[32]), these energy-loss contributions are sign-of-charge dependent (related to odd powers of the projectile nuclear charge). At small impact parameters, the sign of a bare projectile Coulomb-charge is not very important due to a partial cancellation of polarization and binding effect (derived from precision AO-CC results). At these impact parameters, however, the screening of the projectile nuclear charge will introduce another mechanism related to 2nd-order perturbation theory, namely a short-ranged *Barkas (screening-) effect*. The screening influences the mean kinetic electron energy in the projectile field; it leads to a distance-dependent variation of the forces and correspondingly of the electron trajectory.[33] Typically, the net effect is a significant energy-loss enhancement for positive ions. This latter mechanism is already included in the CasP program, using the binary-model ansatz by Sigmund and Schinner[8]. Hence, the close collision fraction of the impact-parameter dependent energy loss[10] $\overline{Q}_0^{close}(b)$ is replaced by the corrected quantity

$$\bar{Q}^{close}(b) = \bar{Q}_0^{close}(b)\frac{2\mathrm{T}_{2b}\left(b,\mathrm{V_p}\right)}{\mathrm{T}_{2b}\left(b,\mathrm{V_p}\right)+\mathrm{T}_{2b}\left(b,-\mathrm{V_p}\right)} \quad \text{(Eq. 1)}$$

where T_{2b} denotes the energy loss in a classical two-body collision using the interaction potential $V_p(r)$ between projectile and target electron (T_{2b} is solved numerically). According to the binary model, the Coulomb part of $V_p(r)$ is also exponentially screened using an adiabatic radius with a screening constant λ . Here, we have used $\lambda = {}^{2v_p}\!/_{\pi\omega}$ in agreement with the polarization treatments of, e.g., Lindhard[33] and coworkers and also Arista and coworkers[34]. This deviates from $\lambda = v_p/\omega$ as used by Sigmund and Schinner[35], whose choice of a screening factor is dictated by the simulation of dipolar interactions in 1st-order perturbation theory, i.e. related to electronic binding and not to the physical concept of charge screening. The atomic polarizability (which depends significantly on details of the target-level structure), however, does not enter this somewhat incomplete Barkas treatment.

II.2 Improved Shell Corrections

The PCA model is not an exact solution of first-order perturbation theory, mainly because it is based on a peaking approximation that erases any influence of momentum-space components. Thus, a corresponding correction, the so-called shell correction, has to be applied. In general, shell corrections account for intrinsic uncertainties of the description of the initial target states and usually also for deficiencies of the treatment of the electron dynamics. Neglecting spatial anisotropies and any dynamic interaction with the target nucleus, one may account for the neglected initial electron-velocity distribution (the shell effect), by using Sigmund's kinetic theory[36], a pure two-body solution. In this work, we use our numerical Hartree-Fock-Slater velocity distribution (not hydrogenic distributions as earlier). The resulting electronic stopping power corrected by the *two-body shell-correction* $S_e(PCA_{2bSC})$ deviates significantly from the uncorrected values $S_e(PCA_{nSC})$, specifically at low velocities.

Fig. 1 displays two types of shell-correction factors as function of the projectile velocity (given in a.u., i.e. in units of the Bohr velocity). The blue circles connected by the dashed curve correspond to $R_{shell}^{2b} = S_e(PCA_{2bSC})/S_e(PCA_{nSC})$, defined above. These data have been determined from the ratio of results based on our CasP energy-loss code[9] (the PCA model for H^++H collisions with an accurate set of oscillator strengths). The solid curve in Fig.1 that connects the red asterisks is a reference result that has been determined under the same condition, showing the ratio $R_{shell}^{exact} = S_e(PWBA)/S_e(PCA_{nSC})$ of the exact PWBA results (exact first-order quantum-perturbation theory for ionization and excitation) and the corresponding PCA results, when all correction terms are switched off.

Fig. 1 shows that both ratios reach 0 at very small speeds and 1 at high speeds. At velocities around 0.7 a.u., both curves cross the 50% value of the ratio. This indicates clear similarities between the two ratios. In other words, the main reason for the shell correction of the PCA is the neglected initial velocity distribution, due to the peaking approximation. However, one may see that there are also significant differences between both curves. The two-body corrections are too low at 1 a.u. and too high at low speeds. This might be due uncertainties in the matching of the different impact-parameter regimes, as introduced in the PCA and UCA product Ansatz. Another very likely reason, however, is the expected failure of the classical two-body correction for slow ions, where the electron–projectile interaction may not be separated from the electron–target interaction (one of the main approximations of Sigmund's kinetic theory[36]).

For an improved shell correction, we use exact PWBA results as a reference. Both ratios in Fig.1 depend on $v_p/\overline{v}_t$ with $\overline{v}_t^2 = \langle v_{HFS}^2 \rangle$. Hence, a shell-corrected energy transfer defined as

$$Q_e^{UCA_{SC}}(b, v_p) = Q_e^{UCA_{2bSC}}(b, v_p) \frac{R_{shell}^{exact}(Z_t, v_p/\overline{v}_t)}{R_{shell}^{2b}(Z_t, v_p/\overline{v}_t)} \quad \text{(Eq. 2)}$$

should improve the final UCA result. Here, the energy transfer $Q_e^{UCA_{2bSC}}$ considers Sigmund's classical two-body shell correction[36] with the full electron-velocity distribution. Further, the influence of the initial binding to the target nucleus as well as uncertainties in the UCA model are considered by the ratio of the two shell corrections determined for a hydrogen-like 1s-target (the ratio of the two curves in Fig.1). We call this type of correction ***shell-effect re-normalization*** and expect it to yield highly accurate stopping cross sections, not only for the target K shell (for hydrogenic K shells, this method yields even exact first-order energy-loss cross-sections). It is noted, however, that both shell-correction terms (R^{exact} and R^{2b}) do not consider the impact-parameter dependence of the excitation/ionization dynamics.

II.3 Improved Electron-Loss Contribution

From atomic physics knowledge, it is clear that capture processes might be very important at low energies. Thus, we consider energy losses during electron-capture and subsequent electron-loss processes in this work. Previous versions of the CasP code include a projectile-electron loss option (for equilibrium stopping powers), but capture processes have not been included so far. Further, asymptotic low-energy kinematics were assumed for the projectile-electron dynamics. Projectile electrons either excited or ionized to low-energy continuum states transfer their momentum to the projectile system, giving rise to maximal energy losses. Fast ejected projectile electrons (with kinetic projectile-system energies ε' that are large compared to the projectile ionization potential I_{loss}), however, do not couple strongly to the projectile nucleus. Following the derivation by Sigmund and Glazov[37], we find a correspondingly reduced stopping cross section

$$S_e^{proj} = S_{e,0}^{proj} - \sqrt{8}\pi v_p \iint \sqrt{\varepsilon'} \frac{d\sigma}{d\varepsilon' d\Omega} \cos\theta \sin\theta \, d\varepsilon' d\theta \,. \qquad \text{(Eq. 3)}$$

Here $S_{e,0}^{proj}$ is the stopping cross section due to electron-loss processes in the projectile frame,

and the simplification $S_e^{proj} \approx S_{e,0}^{proj}$ has been used in most previous investigations.[6, 17] Up to now, Eq. 3 has never been solved accurately, since only very few models yield reliable differential cross sections $d\sigma / d\varepsilon' d\Omega$. For this purpose, we have used colossal basis sets (700 to 1000 projectile-centred states) in AO-CC[27, 28, 29] calculations.

Fig. 2 displays the precise loss correction factor $S_e^{proj} / S_{e,0}^{proj}$ calculated according to Eq.3 as a function of a reduced energy for 4 different collision systems. The abscissa variable stems from an optimization in which we have tried to find a common scaling for the different bound states as a function of $2v_p^2 = 4E_p \frac{m_e}{m_p}$, the maximum energy transfer in a two-body collision. We have minimized the spread between the 4 data sets by fitting powers of the bound state energy I_b and of the mean initial kinetic electron energy $\left\langle E_{kin}^e \right\rangle$. Note that these theoretical results include electron loss as well as also projectile excitation. The solid curve is a least-square fit to these numerical results, which enters all subsequent UCA results. As expected, the correction factor is 1 for low speeds and it approaches zero for projectile velocities exceeding the orbital velocity by far. For the H^++H collision system, we have not only used Eq. 3 (red square symbols) but also the simplified equation

$$S_e^{proj} \approx I_{loss}\sigma_{loss}\,, \qquad \text{(Eq. 4)}$$

as estimated from binary-encounter kinematics[37] (red asterisks), where σ_{loss} is the total electron-loss cross section. It is seen that results from Eq.3 and Eq.4 yield very similar values at low to intermediate velocities. Furthermore, it should be emphasized that the energy-loss contribution drops (the charge-states increase) around the values corresponding to correction factors of 0.5. This means, one cannot neglect the projectile-system correction, but one might use eq. 4 for simplicity.

III. Application of the Improved UCA Model to Rare-Gas Targets

Fig. 3a displays charge-state specific energy-loss cross sections for H+He collisions. The three cases include an active He-target electron and either H^+ or H^0 projectiles as well as an active H^0 projectile-electron perturbed by neutral He. Full colossal-basis AO-CC[27, 28, 29] calculations are compared to the improved UCA. For the electron-loss fraction ($He+H^0$), the UCA uses also the (scaled) fit curve of Fig. 2 and AO-CC results are corrected according to Eq. 3. Since the AO-CC theory includes energy losses due to electron capture in H^++He collisions, an experimental estimate for the electron-capture contribution S_e^{cap} has been added to the UCA. Here we have used

$$S_e^{cap} = \sigma^{cap} \Delta E^{cap}, \qquad \text{(Eq. 5a)}$$

where the cross section σ^{cap} has been taken from existing experimental data,[38] with an estimated energy transfer

$$\Delta E^{cap} = I^{tar} - I^{proj} + v_p^2/2 + \min\left(2I^{proj}, v_p^2/2\right)/4 . \qquad \text{(Eq. 5b)}$$

ΔE^{cap} depends on the static target and projectile ionisation potentials, on the translational energy loss and on an approximate mean dynamic projectile-excitation energy (the last term in Eq. 5b).

The UCA results in Fig. 3a agree to within 30% (for the electron loss) and better with our accurate AO-CC reference results. In Fig. 3b, we show the sum over charge-state averaged UCA energy losses due to inelastic target processes, inelastic projectile processes and electron capture. Experimental data (shown in the figure by red diamond symbols) are taken from the extensive data collection by H. Paul.[39] The comparison shows very good agreement between UCA and experimental data at intermediate to high energies. At low kinetic energies around 5 keV the maximum deviation between experiment and UCA reaches 20%. Fig. 4 displays data similar to Fig. 3b, but obtained for H+Ne, H+Ar and H+Kr. The charge state fractions f_q and

capture cross sections σ^{cap} for these systems have been taken from different sources.[38, 40, 41, 42] It is seen that there is very good agreement between experimental and theoretical energy-loss cross sections. Typical deviations are below about 10%. Consideration of the influence of more deeply bound shells (L1, M1, N1, M45) for the initial-state energy in ΔE^{cap} would further improve the UCA's accuracy (see the upward pointing arrows close to the shell symbols).

IV. Conclusions

In this work, we have extended the UCA energy-loss model by using

- an improved Barkas correction
- highly accurate shell corrections (the new shell-effect re-normalization)
- full kinematics for electron-loss processes
- an experimental estimate of electron capture contributions

which lead to improved stopping-power predictions at low and intermediate energies. Very good agreement between experimental and theoretical results is found here for protons in rare gases. At high energies, this is no surprise, but at low energies this is a big step forward. Further consideration of deeper bound target states for electron capture would bring UCA results and experimental data in nearly perfect agreement for H+Ne and H+Kr. For H+He and H+Ar, there are remaining uncertainties of up to 20% at the lowest energies. The high quality of the current UCA prediction was also proven for partial UCA energy-loss cross sections in comparison to the most precise available AO-CC calculations. Finally, our improved UCA results clearly show that electron capture may not be neglected, leading to strong contributions (25% to 37%, depending on the collisions system) at projectile energies around 40 keV.

Acknowledgements

We acknowledge funding by the Alexander-von-Humboldt foundation, as well as many

interesting discussions with P.Sigmund and many helpful remarks by H.Paul. This work was partially supported by the Brazilian funding agencies CNPq, CAPES and the PRONEX program.

Figures

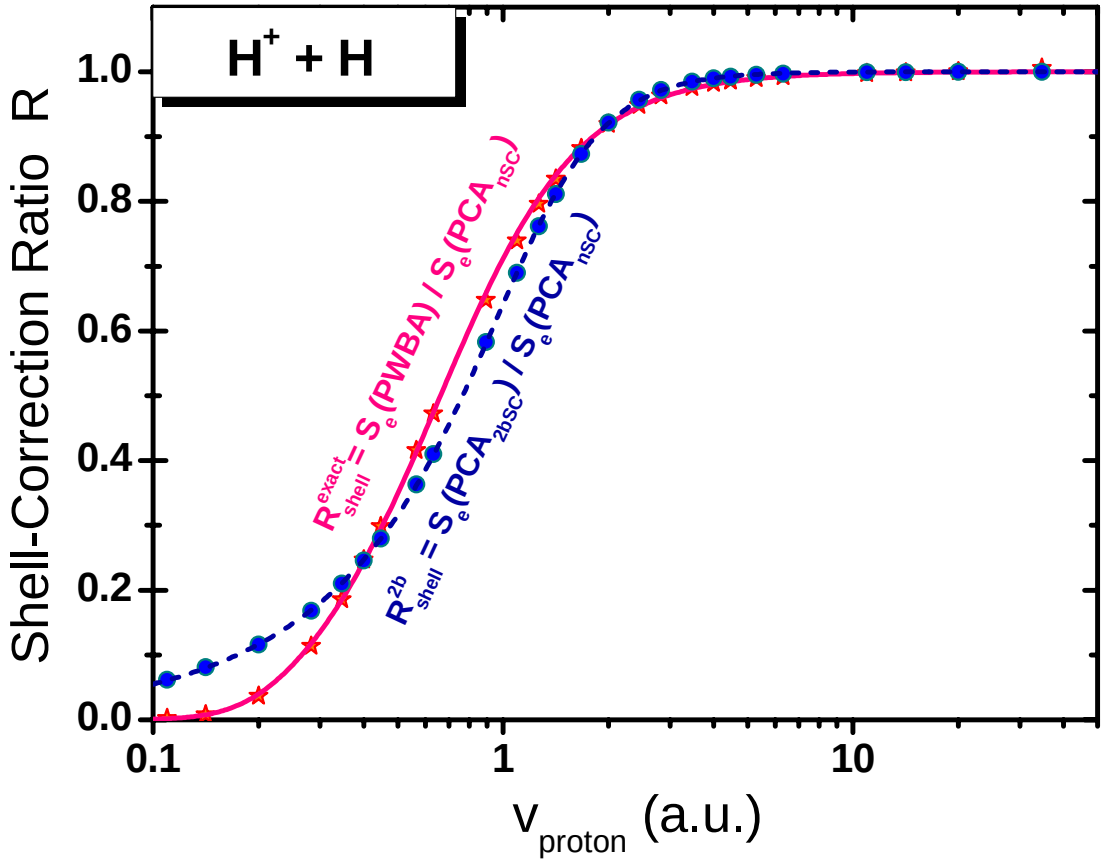

Fig. 1: Two shell-correction types for excitation plus ionization processes in H^+ + H collisions and referring to **PCA**. The ratio R^{exact} (red asterisks and solid least-square fit function) is computed from the "exact" 1st order PWBA stopping cross-sections and impact-parameter integrated PCA values. The ratio R^{2b} (blue circles and short-dashed least-square fit function) is computed from Sigmund's kinematic two-body solution.

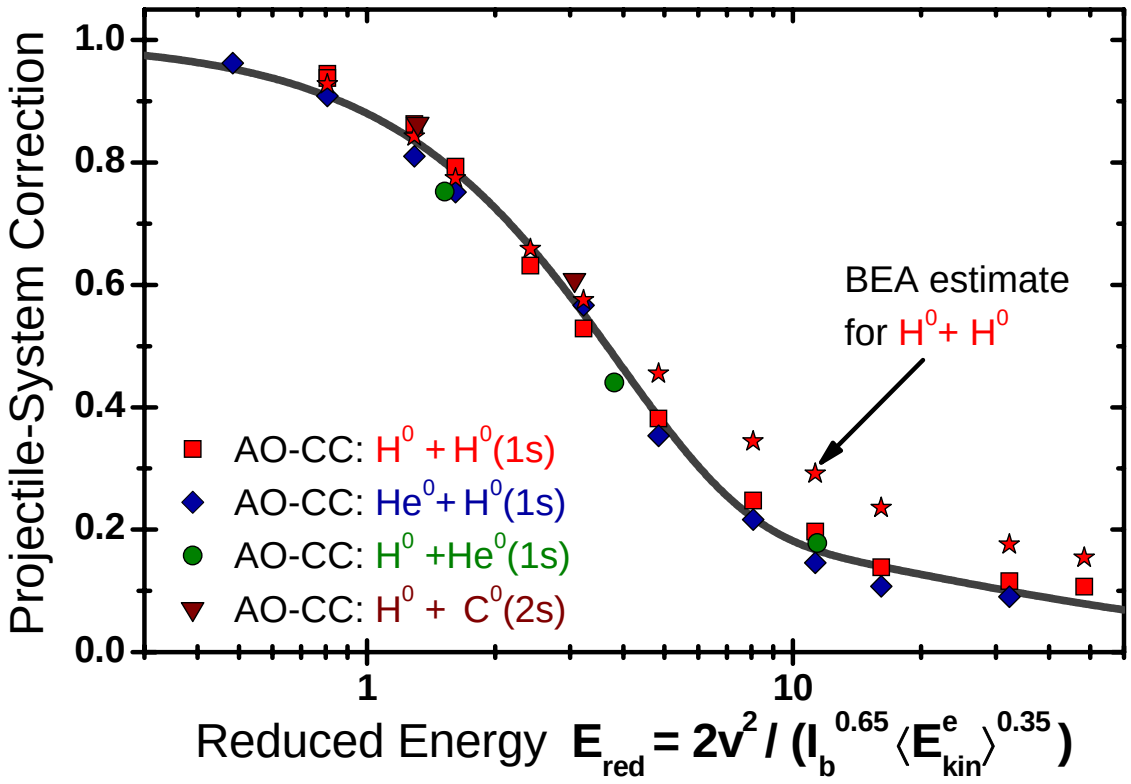

Fig. 2: Reference-frame correction factor for projectile energy-losses due to projectile ionization (electron-loss processes) plus projectile excitation. This factor is evaluated using highly accurate atomic-orbital coupled-channel (AO-CC) results for neutral H and He targets interacting with H-1s, He-1s and C-2s electrons of neutral H, He, and C projectiles. These precision correction factors are given as a function of a reduced energy E_{red}. For one collision system, namely for H^0+ H^0(1s), a subset of the same AO-CC results is used to compute an approximate correction factor (BEA estimate, shown by red asterisks) using Eq. 4.

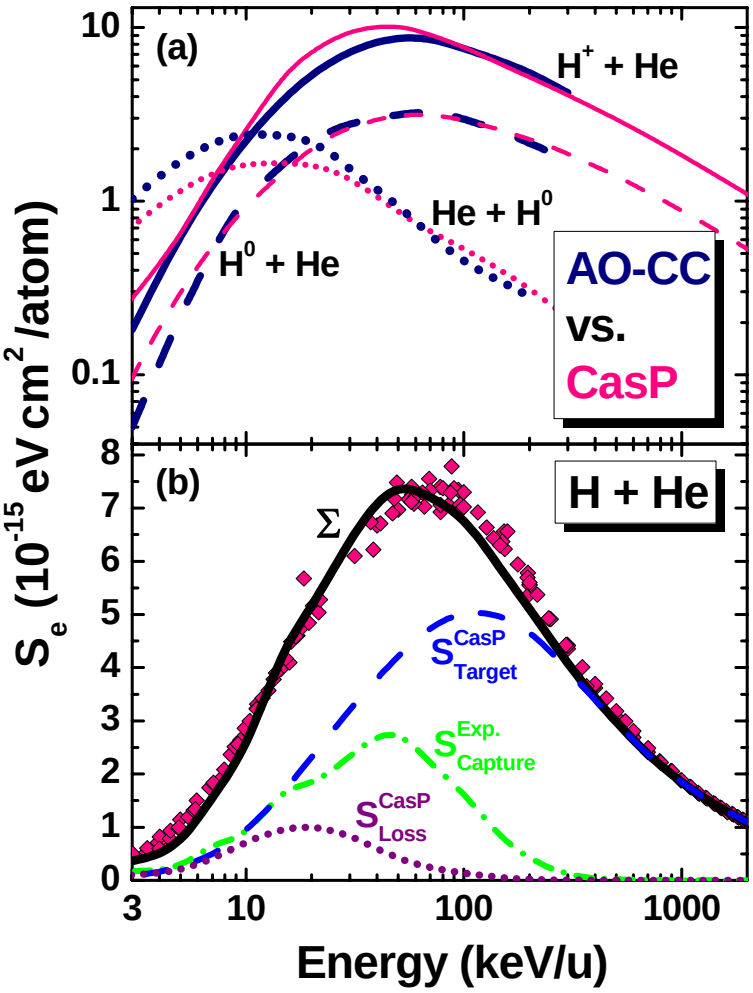

Fig. 3: Projectile-energy dependence of the electronic energy loss of protons in helium gas. Fig. 3a displays theoretical partial energy-loss cross sections (thick curves: atomic-orbital coupled-channel theory and thin curves: CasP model) for specific processes. These processes are excitation, ionization and capture of target electrons (denoted H^++He and H^0+He for the two dominant projectile charge states) as well as excitation and ionization of bound projectile electrons (denoted He+ H^0) including kinematic suppression. Fig. 3b displays dashed, dotted and dashed-dotted curves that are partial energy-loss cross sections for target excitation/ionization, projectile-electron processes and electron capture (determined from experimental data). The curve Σ stands for the total energy-loss cross section. Experimental data (diamonds) are taken from the data collection of H.Paul[39], restricted to values with uncertainties below 10%.

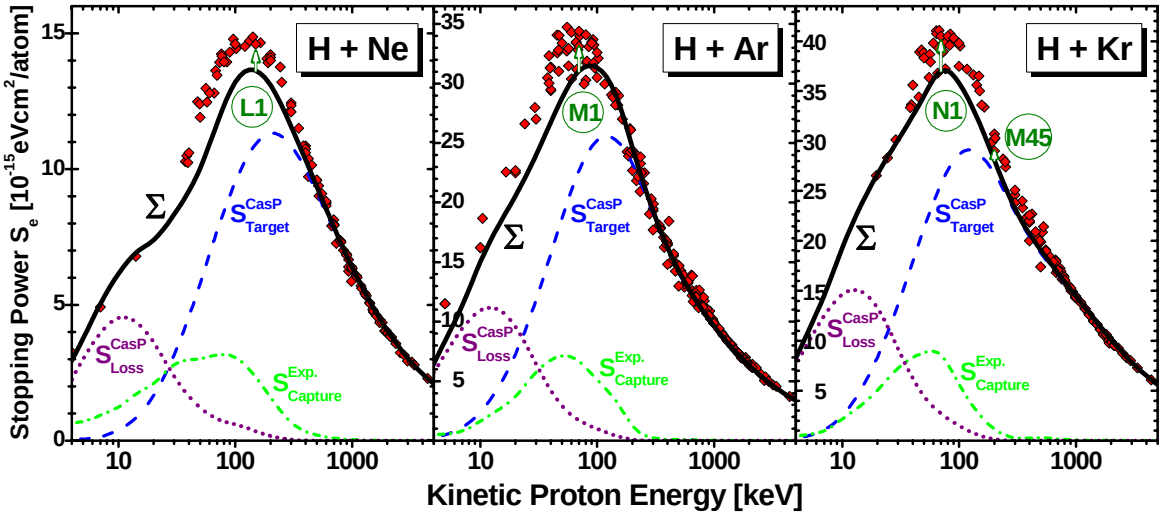

Fig. 4: Projectile-energy dependence of the electronic energy loss of charge-equilibrated protons in different multi-shell rare gases (Ne, Ar and Kr). Experimental values are taken from the data collection of H.Paul[39]. Dashed, dotted and dashed-dotted curves are charge-weighted partial energy-loss cross sections, equivalent to Fig. 3(b). The solid black curve denoted **Σ** corresponds to the sum of these partial contributions. The open arrows and shell indicators (L1, M1, N1, M45) are explained in the text.

References

[1] J.J. Thomson, Phil. Mag. **23**, 449 (1912)

[2] N. Bohr, Philos. Mag. **25**, 10 (1913)

[3] H. Bethe, Ann.Phys. **5**, 325 (1930)

[4] F. Bloch, Ann. Phys. **16**, 285 (1933)

[5] P.L. Grande and G. Schiwietz; in "Advances in Quantum Chemistry", **vol. 45**, pp.7 (ed. by J. Sabin, 2004, Elsevier Inc.)

[6] G. Schiwietz et al., Nucl. Instr. Meth. **B226** (2004) 683

[7] S.A. Cruz , C. Vargas-Aburto, D.K. Brice, E.V. Alonso and D.G. Armour, Phys. Rev. **A27**, 2403 (1983)

[8] P. Sigmund and A. Schinner, Nucl. Instr. and Meth. **B195**, 64 (2002); note that an estimate for electron capture has been included in later stopping calculations of this type

[9] The most recent CasP program version may be downloaded from http://www.casp-program.org/.

[10] P.L. Grande and G. Schiwietz, Phys.Rev. **A58**, 3796 (1998)

[11] P.L. Grande and G. Schiwietz, Nucl. Instr. Meth. **B267**, 859 (2009)

[12] G. Schiwietz and P.L. Grande, Nucl. Instr. and Meth. **B153**, 1 (1999)

[13] P.L. Grande and G. Schiwietz, Nucl. Instr. Meth. **B195**, 55 (2002)

[14] P.L. Grande, G. Schiwietz, Nucl. Instr. Meth. **B136-138**, 125 (1998)

[15] F. Herman and S. Skillmann, in Atomic Structure Calculations, (Prentice-Hall,Inc Englewood Cliffs, New Jersey,1963)

[16] G.M de Azevedo, P.L. Grande, and G. Schiwietz, Nucl. Instr. and Meth. **B164**, 203 (2000)

[17] A. Dalgarno and G.W. Griffing, Proc. Roy. Soc. **A232**, 423 (1955); D.R. Bates and G. Griffing, Proc.Phys.Soc. **A66**, 961 (1953)

[18] T. Kaneko, Phys. Rev. **A33**, 1602 (1986)

[19] H.-D. Betz, Rev. Mod. Phys. **44**, 465 (1972)

[20] J.P. Rozet, C. Stephan, D. Vernhet, Nucl. Instr. and Meth. **B107**, 67 (1996)

[21] G. Schiwietz and P.L. Grande, Nucl. Instr. Meth. **B175-177**, 125 (2001)

[22] J. Bang and J.M. Hansteen, Kgl. Dan. Vidensk. Selsk. Mat. Fys. Medd. **31**, no.13 (1959)

[23] N.M. Kabachnik, V.N. Kondratev and O.V. Chumanova, Phys. Stat. Sol **(b) 145**, 103 (1988)

[24] N. F. Mott, Proc. Cambridge Philos. Soc. **27**, 553 (1931).

[25] M. Inokuti, Rev. Mod. Phys. **43**, 297 (1971)

[26] J.D.Jackson 'Classical electrodynamics' (ISBN 3-11-007415-X, Walter de Gruyter, Berlin, 1981)

[27] G. Schiwietz, Phys. Rev. **A42**, 296 (1990)

[28] G. Schiwietz and P.L. Grande, Nucl. Instr. and Meth. **B69**, 10 (1992)

[29] P.L. Grande and G. Schiwietz, Phys. Rev. **A47**,1119 (1993)

[30] W.H. Barkas, N.J. Dyer, and H.H. Heckmann, **Phys.Rev.Lett. 11**, 26 (1963).

[31] G. de M. Azevedo et al., **Phys.Rev.Lett. 86**, 1482 (2001); L.L. Araujo et al., Phys. Rev. **A70**, 032903 (2004)

[32] George Basbas, Werner Brandt, and R.H. Ritchie, Phys. Rev. **A7**, 1971 (1973)

[33] Jens Lindhard, Nucl. Instr. Meth. **132**, 1 (1976)

[34] Néstor R. Arista, Nucl. Instr. Meth. **B195**, 91 (2002)

[35] P. Sigmund and A. Schinner, Euro. Phys. J. **D12**, 425 (2000)

[36] P. Sigmund, Phys. Rev. **A26**, 2497 (1982)

[37] P. Sigmund and L.G. Glazov, Eur. Phys. J. **D23**, 211 (2003)

[38] S.K. Allison, Rev. Mod. Phys. **30**, 1137 (1958)

[39] Extensive experimental energy-loss tabulations are presented by H. Paul at http://www.exphys.jku.at/stopping/ .

[40] H.Tawara and A.Russek, Rev. Mod. Phys. **45**, 178 (1973)

[41] S.Andriamonje et al., J. Physique **46**, 349 (1985)

[42] M.E. Rudd et al., Phys. Rev. **A28**, 3244 (1983)